

1 **No part gets left behind: Tiled nanopore sequencing of whole ASFV genomes**
2 **stitched together using Lilo**

3

4 Running Title: Tiled amplicon sequencing with improved assembly of African Swine Fever
5 Virus

6

7 Amanda Warr^a, Caitlin Newman^a, Nicky Craig^a, Ingrida Vendelė^{a,♦}, Rizalee Pilare^b, Lilet
8 Cariazo Cruz^b, Twinkle Galase Barangan^b, Reildrin G Morales^d, Tanja Opriessnig^a, Virginia
9 Mauro Venturina^b, Milagros R Mananggit^c, Samantha Lycett^a, Clarissa YJ Domingo^b,
10 Christine Tait-Burkard^{a#}

11

12 ^a, The Roslin Institute and Royal (Dick) School of Veterinary Studies, University of
13 Edinburgh, Easter Bush, Midlothian, UK

14 ^b, College of Veterinary Science and Medicine, Central Luzon State University, Science City
15 of Muñoz, Nueva Ecija, The Philippines

16 ^c, Regional Animal Disease Diagnostic Laboratory, Department of Agriculture Regional Field
17 Office III, City of San Fernando, Pampanga, The Philippines

18 ^d, Bureau of Animal Industry, Department of Agriculture, Visayas Avenue, Diliman, Quezon
19 City, The Philippines

20

21 [♦]Current address: Thermo Fisher Scientific, Vilnius, Lithuania

22 [#] Address correspondence to Christine Tait-Burkard, christine.burkard@roslin.ed.ac.uk .

23 **Abstract**

24 African Swine Fever virus (ASFV) is the causative agent of a deadly, panzootic disease,
25 infecting wild and domesticated suid populations. Contained for a long time to the African
26 continent, an outbreak of a particularly infectious variant in Georgia in 2007 initiated the
27 spread of the virus around the globe, severely impacting pork production and local
28 economies. The virus is highly contagious and has a mortality of up to 100% in domestic
29 pigs. It is critical to track the spread of the virus, detect variants associated with pathology,
30 and implement biosecurity measures in the most effective way to limit its spread. Due to its
31 size and other limitations, the 170-190kbp large DNA virus has not been well sequenced
32 with fewer than 200 genome sequences available in public repositories. Here we present an
33 efficient, low-cost method of sequencing ASFV at scale. The method uses tiled PCR
34 amplification of the virus to achieve greater coverage, multiplexability and accuracy on a
35 portable sequencer than achievable using shotgun sequencing. We also present Lilo, a
36 pipeline for assembling tiled amplicon data from viral or microbial genomes without relying
37 on polishing against a reference, allowing for structural variation and hypervariable region
38 assembly other methods fail on. The resulting ASFV genomes are near complete, lacking
39 only parts of the highly repetitive 3'- and 5'telomeric regions, and have a high level of
40 accuracy. Our results will allow sequencing of ASFV at optimal efficiency and high
41 throughput to monitor and act on the spread of the virus.

42 **Main**

43 African Swine Fever (ASF) is a viral hemorrhagic disease leading to an extremely high
44 mortality of up to 100% within 7-10 days. Clinical signs of infection are non-specific,
45 including fever, ataxia, anorexia, cyanosis, respiratory symptoms, gastrointestinal symptoms
46 and death ¹. The causative agent of ASF is African Swine Fever Virus (ASFV), the only
47 member of the *Asfivirus* genus and the *Asfarviridae* family. The virion is large and complex
48 with a diameter of around 175-215nm containing a large, double stranded DNA genome of
49 around 170-190kb encoding over 150 open reading frames ^{1,2}.

50 ASF is endemic in Africa where a sylvatic cycle between *Ornithodoros spp.* soft ticks and the
51 natural reservoir, African wild suids, maintains its presence ³. Other routes of infection and
52 spread include physical contact, fluids, excretions, contaminated feed and fomites. The virus
53 is extremely resilient and can survive for prolonged periods in a range of environmental
54 conditions in carcasses and pork product. The disease is highly contagious and can be
55 transmitted through relatively low infectious dose in feed and water ⁴. Wild suid species are
56 susceptible to disease but only domestic and feral pigs, as well as Eurasian wild boar show
57 symptoms. ASFV is therefore very difficult to contain.

58 ASF was first discovered in East Africa, with symptoms reported in Kenya in 1914 and the
59 disease described in 1921 ⁵. Outbreaks in other parts of Africa, Europe, Brazil and the
60 Caribbean islands occurred in the 20th century, with African countries being the worst
61 affected. The virus was almost completely eradicated from non-African countries by the end
62 of the century, but an outbreak in the Republic of Georgia in 2007 has since lead to
63 widespread outbreaks in other countries. Since 2018 major outbreaks have been occurring
64 in China, the world's largest pork producer, and it has been reported that up to half of the
65 pigs in the country, representing roughly a quarter of the world's population, died or were
66 culled to contain the outbreak in 2019 ⁶. The spread of the virus in East and Southeast Asia
67 however could not be halted and since further countries including Mongolia, Vietnam,
68 Cambodia, North Korea, Laos and island nations including The Philippines, Indonesia,

69 Timor-Leste and Papua New Guinea have reported outbreaks ^{7,8}. After the initial outbreaks
70 in Eastern Europe and continuing spread, the disease reached the European Union in 2014
71 and continues to spread, not least through the wild boar population ^{7,9}. In late 2020 the virus
72 reached the largest producer of pork in Europe, Germany ¹⁰. The virus is also edging closer
73 to the USA, one of the world's main exporters and importers of pork, having been recently
74 detected in Haiti and the Dominican Republic, only 381km by air from the US territory of
75 Puerto Rico. It is clear, that the disease represents a serious panzootic threat impacting the
76 pork industry and threatening economies already shaken by the SARS-CoV-2 pandemic.

77 To understand the genetic and genomic variation for ASFV, sequencing is primarily focused
78 on a roughly 400bp fragment of the B646L gene, encoding for the major capsid protein p72.
79 This fragment, representing <0.25% of the total genome, is the basis of the current
80 genotyping system, which has identified 24 genotypes so far ¹¹⁻¹⁴. To further discriminate,
81 additional fragments of the E183L gene (p54, ~630bp), CP205L (p30, ~510bp), and B602L
82 (gp83 ~800bp) are used, adding up to less than 1.4% of the genome characterized. Whilst
83 being a DNA virus, antigenic diversity, the ability to acquire large deletions or insertions, and
84 the presence of highly mutagenic hypervariable regions urge the need for whole genome
85 sequencing for virus characterization and epidemiological studies ^{15,16}. To do this at the
86 scale required, there is a need for a cheap and efficient method to sequence the large ASFV
87 genome, whilst high abundance of homopolymers and hypervariable region require highest
88 accuracy ¹⁷.

89 The availability of a portable sequencing technology opens new doors to travel to outbreak
90 locations, sequence, and analyze samples without needing to transport them. The MinION
91 sequencer from Oxford Nanopore Technologies (ONT) can be carried easily in a pocket or
92 carryon bag. This avoids complications of challenging transportation of biological samples,
93 highly contagious agents or the requirement of a cold chain. There is the potential for a fast
94 turnaround from sample collection to analysis, allowing for near live-monitoring of outbreak
95 situations, as observed in during the Western African Ebola virus epidemic 2013-2016, or of

96 course the COVID-19 pandemic. Furthermore, multiplexing and the washing and reuse of
97 the most expensive component of sequencing, the flow cells, allowing for cheaper
98 sequencing than other methods. Finally, the sequencer can produce very long reads which
99 improves assembly potential, particularly of highly repetitive genomes.

100 Whilst it is possible to obtain whole genome sequences of ASFV directly from blood- and
101 tissue extract DNA, the high prevalence of pig DNA and the need for baits or other methods
102 to enrich ASFV DNA render that method inapplicable for high-throughput, fast, sequencing.

103 Here, we present a method to sequence the near complete genomes, excluding only the
104 highly repetitive, variable length telomeric 3' and 5' regions, of ASFV using ONT's MinION
105 sequencing device using a tiled amplicon approach. The genome is amplified in 32 large
106 fragments 7kb in length, amplified simultaneously in two PCR pools. We propose this
107 method as an efficient, highly adaptable, more accurate, fast, and cost-effective option for
108 sequencing of continuing ASFV outbreaks as well as historic samples. We present 10
109 complete ASFV genome assemblies from samples from the early stages of the ASFV
110 outbreak in the Philippines in 2019 assembled either with the tiled sequencing approach or a
111 whole genome sequencing shotgun approach. The portability of Nanopore sequencing
112 makes it ideal for exploring the dynamics of ASFV infections as outbreaks emerge. As ASFV
113 continues to spread around the world, efficient methods of sequencing the genome are
114 essential to improve our understanding of the virus and the ongoing global spread. Our
115 primer sets have been optimized for relatively even coverage and have been designed to
116 bind outside of hypervariable regions. They only anneal to roughly 0.8% of the genome and
117 are designed to be well suited to the current outbreak, able to at least partially sequence
118 other genotypes and be easily modifiable should the virus mutate.

119 Finally, we present the Lilo pipeline. While pipelines exist to assemble genomes from tiled
120 amplicons, they rely on aligning reads to a reference and using polishing tools to generate a
121 consensus from the reads. This method works well for producing a genome sequence with
122 SNPs representative of the sequenced genome, however large indels, structural variants,

123 and hypervariable regions that may be difficult to align to a reference are not accurately
124 represented. For ASFV, whole genes can be inserted or deleted and due to homologous
125 recombination it can carry large structural variations, with indels likely being more important
126 than SNPs in creating viral diversity¹⁸. Therefore, we designed Lilo, which aligns reads to a
127 reference in order to assign them to an amplicon, selects the read with the highest base
128 quality and of the expected length for each amplicon, polishes the read with the remaining
129 reads, removes primers and stitches them together at overlaps ordered and oriented by a
130 reference. This approach makes the pipeline more adaptable to large structural variation and
131 hypervariable regions in genomes than currently available methods.

132

133 **Shotgun sequencing of ASFV directly from blood**

134 In field sequencing, particularly in developing countries, limits the availability of tools and
135 reagents. During the first outbreaks in the Philippines whole DNA was isolated from the
136 highly hemolysed blood collected from ASFV positive pigs. Samples were digested overnight
137 with proteinase K at 55°C prior to phenol/chloroform/isoamyl alcohol extraction and
138 precipitation with isopropanol before washing with 70% ethanol. Whole DNA samples were
139 prepared for sequencing using the ligation sequencing kit (LSK) LSK109 before sequencing
140 samples on a R9.4 flow cell using a MinION mk1b. The data were basecalled and
141 demultiplexed using Guppy (ONT) and the reads assembled with Flye and polished with
142 medaka. (Figure 1A)

143 The time between the beginning of sequencing and detection of the first ASFV read from
144 whole blood ranged from 19 seconds to 3 minutes. As seen in the example of PHL-1969
145 (Figure 1B) the percentage of reads that came from ASFV ranged from 0.006% to 0.24%,
146 likely dependent on the viral titers of the animals culled. ASFV samples show a similar size
147 distribution to other DNA found in the samples, if anything a second small peak of larger
148 fragments can be observed (Figure 1C). All four sequenced blood samples assembled into a

149 whole genome, however, due to variable coverage, the number of mismatches and indels
150 found in some of the samples were high (Figure 3B).

151

152 **Tiled amplicon sequencing of ASFV**

153 Given the low yield of ASFV sequences from shotgun sequencing, as demonstrated by us
154 and others¹⁹⁻²¹, and the high expense per sample, this sequencing approach was not fit for
155 purpose for high-throughput screening of an ongoing virus outbreak. Therefore, we
156 developed a method to amplify, sequence, and assemble ASFV genomes from pigs.

157 In order to enrich ASFV from the sample easily, a PCR amplification approach was chosen,
158 due to its ease of use and usually readily available tools in many countries and labs. Tiling
159 primers were designed targeting 7kb amplicon length and 1kb amplicon overlap using primal
160 scheme using a set of 26 ASFV reference sequences (Figure 2A). The primers are well
161 suited to genotype II, from the current outbreak, but also cover the majority of the genome
162 for at least genotypes I and IV (Figure 2B). This relatively long amplicon size was chosen to
163 reduce the number of primer pairs but also to span potential hypervariable regions. After
164 initial individual performance tests, several primers were redesigned from the original set of
165 primers produced by primal scheme, however the majority of them worked well from the
166 beginning. Fragments were amplified using the PCRBio VeriFi Hot Start high fidelity
167 polymerase according to the manufacture's instruction. Following redesign, all primers
168 amplified their targets, however, they did so at different efficiencies leading to uneven
169 coverage over the genome. To test this, evenly concentrated pools of primers (pool 1 and
170 pool 2, Figure 2A and Figure 2C) were used to amplify blood DNA extract samples from
171 ASFV-infected pigs. Following initial amplifications, pools were split into three pools with
172 primer pair 1, producing a shorter 4kb fragment continuously outperforming the others in a
173 mixed reaction on its own, and primer concentrations in pool 1(Pair 1) and pool 2 were
174 gradually adjusted according to their performance. PCR products per sample were

175 combined, libraries prepared using the LSK109 kit in an R9.4 flow cell. Figure 2D
176 demonstrates the improvement that can be gained by tweaking primer concentrations from
177 evenly represented primer pairs (purple) to optimized primer concentrations (green). These
178 optimizations improve performance for multiplexing of multiple samples on one flow cell.

179 Fresher samples amplify more cleanly, but older, degraded samples will still amplify
180 sufficiently. To show this, we highlight two samples; sample PHL-126, which has been
181 heavily used and degraded, and sample PHL-261, which has been used less frequently
182 (aliquot stored in freezer without frequent use) and is of better quality. As can be seen in the
183 automated electrophoresis result of a tapestation (Figure 2E), PHL-126 shows poor
184 amplification and relatively many amplicons <7kb. Good amplification can be seen for the
185 shorter amplicon pair 1 still. PHL-261 on the other hand shows continued good amplification
186 of the desired 7kb and 4kb products of pool 1 (odd), pool 2 (even) and pair 1, respectively.
187 These samples were prepared with the LSK109 kit and multiplexed using native barcoding
188 and run on a R9.4 flow cell with 3 other ASFV genomes having been pooled in
189 representative quantities, the poorer amplification of PHL-126 had lower sequencing
190 throughput than the better quality PHL-261, but was still assembled into a near-complete
191 genome. Figure 2F shows sequencing coverage of the same two samples and the
192 proportion of total reads for each that was assigned to each of the 32 amplicons.

193 The post-amplification DNA Integrity Number (DIN) can be used to help predict
194 multiplexability, as different quality samples will impact the needed throughput. Figure 2G
195 shows the relationship between the post-amplification DIN and throughput <3kb, and Figure
196 2H demonstrates the number of gaps for different throughputs of reads >3kb. Samples PHL-
197 126 (orange) and PHL-261 (blue) have been highlighted in pale (super accuracy base calling
198 (SAC)) and strong (high accuracy base calling (HAC)) colors, respectively. Figure 2H
199 demonstrates the required throughput per sample and the gaps that can be expected in
200 genomes produced with lower throughputs. Assuming a theoretical MinION throughput of
201 30GB, it should be possible to multiplex over 24 samples, and potentially up to 48 samples

202 (including PCR control), however we would recommend starting with fewer and assessing
203 achievable throughput for each sequencing location as there is variability in expected
204 throughput between users, flow cells, and geographical location. The integrity of the sample
205 will also impact the throughput with degraded samples leading to sequencing capacity being
206 taken up by shorter fragments instead of the required full length amplicons (Figure 2G). For
207 very poor samples, more stringent size selection with AMPure XP beads prior to sequencing
208 may be necessary if samples are to be multiplexed. While it is impractical to run an
209 automated, high resolution electrophoresis, such as a tapestation, after every amplification,
210 users can test a typical sample type (e.g. from decomposing wild boar, from farm culled pigs,
211 with/without cold chain) to predict the likely multiplexability and clean-up steps of similar
212 samples.

213

214 **Lilo assembly of genomes from tiled amplicons**

215 Comparing ASFV genomes we found major variation of the genome often originating from
216 indels. Available assembly pipelines were struggling with such variation when it did not
217 correspond to the reference sequence. Therefore, we developed the Lilo pipeline (Figure 3A)
218 to assemble the tiled amplicons (<https://github.com/amandawarr/Lilo>). Whilst Lilo uses a
219 reference alignment to sort the amplicons, it polishes against the highest quality reads rather
220 than a reference sequence. Using this pipeline, highly accurate genomes were obtained with
221 mismatch accuracy approaching Q50 when using SAC (Figure 2I) and indel accuracy up to
222 Q40 when compared to a closely related publicly available ASFV genome assembly
223 (MN715134.1)²¹, which may still be quite divergent from these samples in truth.

224 QUAST²² (v5.0.2; quality assessment tool for genome assemblies) results demonstrate that
225 the increased coverage of the tiled amplicons produced a more accurate assembly than
226 shotgun sequencing of the virus using a whole flow cell sequencing directly from extracted
227 DNA. Shotgun sequencing however, was able to highlight some samples with longer

228 telomeric regions, such as PHL-237, which is a clear advantage of long-read sequencing
229 technology and something that should be explored for more in-detail investigations into the
230 role of the ASFV telomeric regions. Overall, SAC produced fewer mismatches and indels
231 than HAC and should be the preferred method, however, the time for base calling is a trade-
232 off. Samples with high percentages of unassigned bases (N's) clearly correspond to DIN
233 numbers (Figure 3B).

234 The assembled genomes had excellent agreement on genome structure with the same
235 samples assembled from shotgun sequencing (Figures 3B & 3C). The repetitive content
236 shown at the edges of Figures 3B and 3C are sequences from the telomeres, showing that
237 despite the sequences being from tiled amplicons, they do cover the majority of the genome
238 and part of the telomeres.

239

240 **Accuracy of Lilo and ARTIC assembled genomes**

241 We assessed the quality of Lilo assemblies against those produced with the ARTIC pipeline
242 (v1.2.1). A selection of the ASFV sequencing data were assembled using the ARTIC
243 pipeline, as well as using Lilo, both using the assembled shotgun sequence PHL-1969 as a
244 reference.

245 QUAST analysis shows lower numbers of mismatches against the closest reference
246 (MN715134.1) but higher indels. The percentage of unassigned bases is much higher for
247 ARTIC at around 2.4% whereas Lilo is at 0 or nearly 0%.(Figure 3B)

248 Comparing Lilo-assembled genomes and ARTIC-assembled genomes to a reference
249 (MN715134.1) a number of indels can be observed. Figure 4A shows a likely real indel in the
250 PHL ASFV samples which all assemblies agree on and which is well supported by the reads.
251 In contrast, Figure 4B shows the only indel unique to almost all of the assemblies produced
252 by the Lilo pipeline while being absent from all artic assemblies and occurs in a
253 homopolymer, Most reads appear to support the deletion assembled by Lilo, whether this is

254 a real sequence or a result of poor accuracy of Nanopore sequencing of homopolymeric
255 regions is a more difficult question. Figure 4C shows an extreme example of a very long
256 homopolymeric region, ASFV has several of these and typically neither assembly method
257 agrees on the length of the homopolymer, with the reads lending no strong support to either
258 assembly. While errors from the Lilo pipeline tended to be randomly dispersed among
259 homopolymers, ARTIC errors tended to be more systematic, appearing consistently across
260 the assembled genomes. Frequently, homopolymers lead to the ARTIC pipeline replacing
261 the base immediately before the homopolymer and the first base of the homopolymer with a
262 pair of N's, as can be seen in Figure 4E and 4F. There were also occasions when reads did
263 not support an indel, and there wasn't a clear cause of an indel in the reads or reference, as
264 can be seen in Figures 4D and 4E. There are several of these types of indels throughout the
265 assembly, where Lilo assemblies better agree with both the reads and the reference, likely
266 contributing to the lower QUILT scores of ARTIC on homopolymers and the percentage of
267 undefined bases.

268

269 **Phylogenomics**

270 A maximum likelihood phylogenomic tree was constructed incorporating the newly
271 assembled genomes from tiled data of R9.4 flow cells with HAC with publicly available whole
272 genome ASFV sequences using iqtree (v2.0.5; Figure 5A), and for B646L gene, encoding for
273 the major capsid protein p72, genotype II sequences specifically (Figure 5B).

274 As observed in Figure 5A, p72 genotypes do not correspond to the clustering. For example,
275 the E75 strain Spain 1975 isolate, an early genotype II, is grouping with genotype I's.

276 Unfortunately, the phylogeny contains many gaps and lacks both timely and geographic
277 resolution, showing that much more sampling is required. PHL samples clearly cluster within
278 the highly virulent, novel p72 genotype II cluster.

279 Resolving the tree further, selecting only those clustering with the novel p72 genotype II
280 genomes two distinct clusters of PHL sequences can be observed. Whilst, due to the
281 similarity of the genomes, the orders of lower branches are of lower confidence than those of
282 higher branches, reanalysis still suggest two different introductions into the Philippines
283 (internal branch lengths may be found in supplementary documents S1 and S2). Whilst
284 indications are that one cluster is closer related to Asian isolates, the other one showing a
285 more likely Eastern European origin, the lack of sample numbers to fill branch gaps and
286 common ancestors makes conclusive interpretation impossible.

287 Discussion

288 ASFV is a serious threat to the global pork industry and consequences of depopulation,
289 reduced availability of pork, and increased prices of other animal protein affect local
290 economies, especially in low- and middle income countries with high reliance on pig protein.
291 Tracing the spread of the virus, understanding more about genome-pathology links, and
292 consequently implementing targeted biosafety measures are paramount to combat the
293 disease. As demonstrated in Figure 5, current genotyping methods based on partial
294 sequencing of the B646L gene, encoding for the major capsid protein p72, do not
295 correspond to whole-genome sequencing and are therefore inadequate to trace virus
296 evolution.

297 Here, we have demonstrated an efficient method for sequencing the ASFV genome. Despite
298 the use of tiled amplicons, part of the 3'- and 5' telomeric regions of the virus are included in
299 the tiled amplicon assemblies, meaning the majority of the genome is included.

300 As demonstrated by us and others, ASFV sequences can be obtained by direct sequencing
301 from blood or other tissue samples of infected pigs¹⁹⁻²¹. The resulting sequence includes
302 interesting information on the lengths and repeats found in the telomeric regions, which may
303 be helpful for more in-depth investigation into the virus pathology and spread. However,
304 without enrichment for ASFV¹⁷ or depletion of host-methylated DNA²³ sample percentage
305 for ASFV is low relative to host DNA in the samples, meaning that obtaining sufficient ASFV
306 reads to assemble the genome from shotgun sequencing usually requires an entire MinION
307 flow cell, or more, depending on viral titer and original sample type. Bone marrow or blood
308 will likely yield the best virus:host ratio with spleen or muscle, whilst good sources of viral
309 DNA²⁴, also contain a large number of nucleated host cells. Even if sufficient data is
310 obtained to assemble the genome, the coverage is likely too poor to sufficiently polish the
311 genome. In contrast, the tiled amplicon method can be used on samples with lower viral
312 titers or degraded DNA, selectively sequences the virus, and can be multiplexed on a flow
313 cell to simultaneously sequence multiple samples at high enough coverage for good

314 polishing. Especially in countries where ASFV is circulating in wild boar or feral pigs,
315 samples may be collected from infected animals that have been dead for a prolonged period
316 of time. It is important that the method is capable of amplifying virus from both high- and low
317 quality samples. Figure 2E demonstrates the variability of DNA integrity post-amplification
318 and that even poor samples that have been degraded amplify and produce near complete
319 genome assemblies.

320 Overall, the PCR amplification method increases coverage, is less prone to exhaust flow
321 cells quickly, allows for multiplexing, and consequently reduces costs, improves genome
322 accuracy, and removes the need for specialized enrichment or depletion methods.

323 Whilst ~7kb amplicons are very large compared to other comparable methods for other
324 viruses, the size of the ASFV genome, the stability of DNA, the relatively low numbers of
325 primer pairs, and the advantages of long reads detecting recombinants more easily make
326 this the best approach. Especially with the small, medium, and large indels that can occur in
327 ASFV¹⁸, it is important to get good resolution across these regions, which can be achieved
328 easily with large amplicons. It is important though to choose the right, high accuracy
329 polymerase capable of amplifying such long amplicons. We found PCRBio VeriFi to be
330 highly capable of this with the hot start version producing very few non-specific products,
331 whilst the non-hot start version can produce more non-specific product, which may be an
332 advantage for variant testing. As demonstrated in Figures 2E and F and 4B show that even
333 low quality samples can produce whole genome assemblies with few gaps. However, a
334 limitation of the large tiled amplicon method is that should a variant occur at the site of a
335 primer, the amplification of a relatively large section of genome will fail. While this is an
336 inconvenience, it will be simple to redesign a primer to replace the failed one or to act as an
337 alternate primer. It is also possible to amplify across a larger region using the existing
338 primers either side of the failed one, generating a 14kb product, to sequence a larger region
339 and design a primer from the sequenced amplicon. This was found to be possible using the
340 VeriFi HS polymerase and allows for the method to adapt as the virus changes.

341 Whilst Nanopore sequencing methods provide a lot of advantages, such as sequencing on
342 site, portability, and accessibility to less specialist communities, there are, as for any
343 sequencing method, drawbacks.

344 As demonstrated in Figure 1I & 1J the choice of flow cell and basecalling method has an
345 impact on the accuracy of SNPs and indels. Generally, throughput is lower and required
346 input DNA is higher for R10.3 flow cells, however HAC on R10.3 is of comparable accuracy
347 to SAC on R9.4, with super accuracy on R10.3 being of even higher quality. SAC is very
348 slow and resource hungry, and when speed is important such as in an active outbreak,
349 R10.3 with HAC may be a good compromise for maximising efficiency with minimal sacrifice
350 of accuracy. However where the highest accuracy is required we recommend using R10.3
351 flow cells and basecalling with a super accuracy model.

352 All of our assemblies have indels compared to the reference partially stemming from
353 systematic errors in Nanopore sequencing in the abundant homopolymers and repeats in the
354 ASFV genome (e.g. PHL-1969 contains 6.8% homopolymers of 4bp or more), however with
355 the latest kits and flow cells from Nanopore, and without additional costs, we would expect
356 future developments to continually reduce the indel errors without major alterations to the
357 wet or dry lab methodologies described here. Additionally, some indels are likely true
358 variations, and in many cases these indels are clearly present across all of our genomes
359 (Figure 4A), and are not in homopolymeric regions, suggesting true variation between
360 samples and the reference used. Additional sequencing of the same amplicons with a higher
361 accuracy technology, such as Illumina could be used to polish the assemblies, however this
362 would add time and cost. Reducing the number of false indels, where possible, is important,
363 as the ASFV genome is known to have functionally relevant indels²⁵. Polishing with an
364 accurate reference can produce assemblies that are very accurate, however, these methods
365 do not handle structural variants and hypervariable regions well. While the genomes
366 sequenced here do not have any major indels compared to the reference used, diversity in
367 ASFV is partially driven by small, medium and large indels¹⁸ and increased sequencing of

368 samples is likely to reveal more of them. While errors from the Lilo pipeline tended to be
369 randomly dispersed among homopolymers, ARTIC errors tended to be more systematic,
370 appearing consistently across the assembled genomes. Errors occurring in the same
371 position between genomes may be more likely to impact phylogenomic analysis than
372 relatively random errors. The only consistent indel error found across the majority of the Lilo
373 assembled genomes that was always absent in the artic genomes is shown in Figure 4B.
374 This region contains a homopolymers, which is typically difficult to correct from Nanopore
375 sequencing data, however while the ARTIC assembly more closely agrees with the
376 reference, the reads are well-supporting of the deletion found in the Lilo assemblies. It is not
377 unusual when carrying out multi-sequence alignments between whole ASFV genome
378 sequences, even those constructed from reads from a higher accuracy sequencing
379 technology, to find large homopolymers of variable length and it is unclear to what degree
380 these are limitations of sequencing technologies as opposed to real variation.

381 The Lilo pipeline also has some limitations, it currently assumes that any structural variants
382 will not change the length of any given amplicon by more than 5%, it assumes that structural
383 variants will not be dramatic enough to prevent alignment to the reference for the purposes
384 of assigning reads to amplicons and ordering and orienting the polished amplicons. Lilo also
385 assumes the reads will be the full length of the amplicon, making it incompatible with ONT
386 rapid kits that utilize transposases. However, the strength of not relying on polishing reads
387 aligned to a reference is beneficial for genomes where structural variation is expected to be
388 important, and for species with hypervariable regions which may not align and polish well
389 with a reference. The pipeline has been tested on tiled sequences from ASFV, Porcine
390 Reproductive and Respiratory Syndrome-1 & -2, and SARS-CoV-2 (data not shown here)
391 and can handle custom schemes for other viruses.

392 ASFV is very under-sequenced with only a small number of whole genome sequences
393 available and there is a need for an affordable way to sequence the virus at scale, as
394 previously discussed ¹⁷. While the majority of sequences produced from sequencing

395 individual genes in the virus have been frustratingly similar ²⁶ reducing their usefulness in
396 epidemiological studies, variants and large deletions have been observed across the
397 genome, and these have been found to affect phenotypes ²⁵. As outbreaks continue to
398 spread around the world and the amount of virus in circulation increases, these variations
399 will likely increase in frequency. Additionally, there are few of the ancestral viruses from
400 Africa sequenced, and these should be sequenced to understand the evolution of ASFV,
401 particularly the loss of its dependence on the sylvatic cycle. Given the slow mutational rate of
402 the virus, sequencing individual genes is unlikely to be informative and so to have a chance
403 of seeing variants in the virus the whole genome must be sequenced. The ability to amplify
404 the genotypes with our current scheme decreases with distance from genotype II, and
405 additional primers will need designing in the future to improve coverage over other
406 genotypes, however current coverage using this primer scheme is still likely to be of more
407 use than the p72 gene alone. Coverage gaps can be resolved relatively easily as larger
408 amplicons can be generated with flanking primers. Should primers on older or emerging
409 samples fail, the altered region can be amplified using primers from either side of the failed
410 amplicon, spanning the region, and the sequenced amplicon can be used to design new
411 primers for the region.

412 Phylogenetic trees of currently available whole-genome ASFV sequences highlight the
413 inadequacy of the p72 genotyping in reflecting similarities of ASFV on a genomic level. The
414 sparsity of whole-genome sequences hampers the ability to trace virus movement and
415 results in high levels of uncertainty in phylogenetic analyses. Running the maximum
416 likelihood tree analysis including the whole-genome sequences obtained from tiled
417 amplification in this manuscript reliably grouped samples from the early Philippines outbreak
418 of ASFV in November 2019 into two clusters. This indicates at least two potential
419 introductions of ASFV into the Philippines. Due to the lack of samples and resolution in the
420 phylogenetic tree, no conclusion about countries or region of origins is possible.

421 We have presented an efficient, low cost method for sequencing and assembling ASFV
422 which can be carried out in the lab or in the field during outbreaks. The Lilo pipeline is a
423 lightweight pipeline that can be run on a standard laptop with 16GB RAM and no internet
424 connection, making it ideal for in field bioinformatic analysis of ASFV and other viruses.

425 **Methods**

426 **Samples**

427 Blood samples from outbreaks in central Luzon (Philippines) were collected following
428 depopulation of pigs within a defined containment radius. Blood samples were tested for
429 ASFV by PCR. Blood samples from ASFV-positive pigs were pooled at equal amounts by
430 farm before further processing.

431 **DNA extraction**

432 Blood samples were spun for 20min at 3,000rcf before decanting the supernatant. 5xTEN
433 buffer(0.05M EDTA, 0.5M NaCl, 20mg/ml Proteinase K, 20% SDS, in 0.05M Tris-HCl,
434 pH8.0) were added to a 1x final concentration before incubation overnight at 55°C in a
435 shaking water bath. Equal volumes of phenol were added and gently mixed. Following 20min
436 centrifugation at 3,000rcf the aqueous phase was transferred to a fresh tube. If the phase
437 was very viscous, the phenol phase was re-extracted to improve yields. An equal volume of
438 phenol/chloroform/isoamyl alcohol (25:24:1) was added to the aqueous phase before mixing
439 and separation by centrifugation, 10min, 3,000rcf. The aqueous phase was transferred to a
440 fresh tube before addition of 1:10 3M sodium acetate and an equal amount of isopropanol.
441 Following 1h incubation at -20°C, samples were spun for 10min at 16,000rcf before washing
442 the pellet with 70% Ethanol. The pellet was dried and resuspended in nuclease-free water.

443 **Nanopore sequencing directly from DNA extracted from blood in the Philippines**

444 Samples were sequenced following Nanopore's SQK-LSK109 protocol on R9.4 flow cells on
445 a MinION mk1b. The protocol was started with 1ug of DNA as measured on an Implen
446 NanoPhotometer P330. The protocol was carried out as recommended by ONT with the
447 following modifications: The 20°C and 60°C incubations after the addition of NEB's FFPE
448 repair and End-prep reagents were done for 30 minutes at each temperature instead of 5
449 minutes, and the room temperature incubation for the ligation reaction was done for 20
450 minutes instead of 10. During sequencing, two USB desk fans were pointed at the MinION to

451 assist with maintaining appropriate temperature for the run in the above average “room
452 temperature” in the lab in the Philippines.

453 **Designing primers for tiled amplification**

454 Tiled primers were designed using Primal Scheme (v1.3.2)²⁷. A set of 28 complete African
455 Swine Fever genomes (listed in Supplementary Document S3) were downloaded from NCBI
456 for primer design, which at the time were all that were available. Additionally three Filipino
457 whole ASFV genomes we had assembled from shotgun sequencing data were included. A
458 multi sequence alignment was carried out with Clustal Omega (in MEGA v7.0.2)²⁸. Primal
459 Scheme was run to produce 7kb amplicons with 1kb overlap resulting in 32 overlapping
460 primer pairs in two non-overlapping pools. Primers were tested on samples and while the
461 majority worked first time, several had to be redesigned due to failed amplification or
462 preferential amplification of off-target regions. Redesigns were done using Primer-BLAST²⁹,
463 targeting a similar region of the genome to the failed amplicon. Some primers amplified more
464 efficiently than others and in order to make the coverage of these as even as possible, some
465 primers were tweaked to have a different concentration. One primer pair (amplicon 1) was
466 shorter than the others in order to avoid highly repetitive sequence in the telomeres and it is
467 recommended to amplify it in a separate reaction to pools 1 and 2 to avoid
468 overrepresentation.

469 **Amplification, library prep and sequencing of tiled amplicons**

470 Tiled primers were initially tested individually at 200nM concentration using approximately
471 90ng ASF DNA and Phusion High-Fidelity PCR Master Mix with HF Buffer with 1mM added
472 MgCl₂ (both New England Biolabs, Ipswich, MA, USA). Individual PCRs, in a 25µl reaction
473 volume, underwent initial denaturation of 2 minutes at 98°C, followed by 33 cycles of 10
474 seconds at 98°C, 30 seconds annealing at 63°C, and 4 minutes and 40 seconds extension
475 at 72°C, followed by a final extension for 10 minutes at 72°C. PCR products were then
476 examined using Tapestation Genomic DNA analysis (Agilent, Santa Clara, CA, USA). While

477 a small amount of off-target amplification was tolerated, primers which produced strong off-
478 target bands or weak bands of the correct 7kb size were redesigned.

479 Once the complete set of primers had been successfully designed to cover the complete
480 genome, the primers were pooled in equal amounts into two pools of non-overlapping
481 primers. These pools were tested using the same conditions as the individual PCRs, but in a
482 50 μ l reaction volume and using 1 μ M of the primer pool. The resulting PCR products were
483 cleaned using 0.4 \times volume AMPure XP beads (Beckman Coulter, Indianapolis, IN, USA) to
484 remove products smaller than approximately 2kb in length, then pooled equally prior to
485 sequencing. The cleaned PCR products were quantified using a Qubit ds DNA BR assay
486 (Invitrogen, Waltham, MA, USA) and combined in equimolar amounts to a total of 700ng for
487 library preparation according to the Native barcoding genomic DNA (with EXP-NBD104,
488 EXP-NBD114, and SQK-LSK109)-Nanopore protocol.

489 Following bioinformatic analysis of sequencing data, primers which were found to be over- or
490 under-performing were either redesigned or their contribution to the pool was adjusted
491 accordingly, and the new primer pool tested as above in an iterative fashion. Ultimately 2
492 non-overlapping pools and a separate reaction for primer pair 1 were used to obtain the
493 most even coverage and were processed as above, and pooled proportionally to the number
494 of amplicons in each pool prior to sequencing. Additionally the polymerase was swapped
495 from Phusion to VeriFi (PCRBIO) in a 25 μ l reaction using 2 μ l DNA per reaction, which has
496 markedly better performance on the amplicons with far less off-target amplification. The PCR
497 conditions for this polymerase were an initial denaturation of 1 minute at 98 $^{\circ}$ C, followed by
498 40 cycles of 15 seconds at 98 $^{\circ}$ C, 15 seconds annealing at 60 $^{\circ}$ C, and 4 minutes and 40
499 seconds extension at 72 $^{\circ}$ C, followed by a final extension for 5 minutes at 72 $^{\circ}$ C. AMPure XP
500 bead cleanup after PCR is optional, but recommended in samples with low DIN. Primer
501 sequences, recommended primer concentrations and recommended pooling quantities are
502 described in supplementary table S1, and any updates to these will be released on Lilo's
503 github page.

504 Samples were sequenced following Nanopore's SQK-LSK109 or SQK-LSK110 protocol on
505 R9.4 or R10.3 flow cells (which combination is specified alongside relevant results) on a
506 MinION mk1b or mk1c. The protocol was started with 1ug of pooled amplicons as measured
507 on a qubit using broad range reagents. For samples using multiplexing, the native barcoding
508 expansion kit from Nanopore was used following Nanopore's instructions when using SQK-
509 LSK109. For using the barcodes with SQK-LSK110, the instructions for SQK-109 were
510 followed until after the barcodes had been ligated on, at which stage the end prep was
511 repeated and we follow the standard protocol for library prep with SQK-LSK110 from after
512 the end prep step.

513 **Bioinformatic processing of ASFV genomes sequenced with shotgun sequencing**

514 The data were basecalled and demultiplexed using MinKNOW (v19.06.8; ONT) using "fast"
515 basecalling. Following basecalling the reads were aligned to an ASFV genome using
516 minimap2 to identify ASFV reads, the fast5s for these reads were extracted using
517 fast5_subset from the ont_fast5_api (https://github.com/nanoporetech/ont_fast5_api) and
518 these were basecalled again using high accuracy basecalling. This was done to reduce
519 basecalling time, as this work was done locally in the field on a laptop without a GPU. The
520 reads were assembled with Flye (v2.6)³⁰ and polished 3 times with Medaka (v0.7.1; ONT).
521 Comparisons of quantity of data produced and the proportion of which were ASFV reads
522 were done using NanoComp (v1.28.1)³¹.

523 **Bioinformatic processing of ASFV genomes from tiled amplicons with Lilo**

524 The data were basecalled and demultiplexed using Guppy (v5.0.14; ONT) using high or
525 super accuracy model on a GPU. The snakemake pipeline, Lilo
526 (<https://github.com/amandawarr/Lilo>), was developed and as summarised in Figure 3A,
527 takes the following steps:

- 528 1. Use Porechop (v0.2.3) to remove any sequencing adapters or barcodes that have
529 made it through demultiplexing.

- 530 2. Align to a reference with minimap2 (v2.22)³² and samtools (v1.12)³³ and separate
531 reads into amplicons by alignment position with bedtools (v2.30.0).³⁴
- 532 3. Select reads of the expected amplicon length (+/-5%) and subset to 300X
- 533 4. Select the read with highest average base quality within +/-1% of the median length
534 of reads for the amplicon to be the “reference” (with bioawk v1);
535 <https://github.com/lh3/bioawk>), remove any amplicons with fewer than 40 reads.
536 Targeting the median length allows for flexibility for large insertions or deletions.
- 537 5. Pool amplicon reads and references back into their original non-overlapping pools.
- 538 6. Polish the pools 3x with medaka (v1.4.4; ONT) and combine resulting polished
539 amplicons.
- 540 7. Align to the reference with minimap2 and remove soft clipped bases (these likely
541 represent missed barcodes or adapters)
- 542 8. Run porechop (specific fork: <https://github.com/sclamons/Porechop-1>) to remove
543 primers from the amplicons.
- 544 9. Merge the amplicons with scaffold_builder (v2.3)³⁵.

545 The required input to Lilo are demultiplexed reads in fastq format in a directory named
546 “raw”, a reference fasta, a bed file of primer alignments (as output by primal scheme), and a
547 csv of primer sequences (if there are ambiguous bases it is advised to expand them first)
548 and a config file, described on the github page. It is adaptable to any species (with a single
549 genome fragment/chromosome) with any tiled primer scheme. The pipeline outputs a fasta
550 file containing the assembled genome.

551 **ARTIC assemblies**

552 A subset of genomes were also assembled using the Artic pipeline
553 (<https://artic.network/ncov-2019>; v1.2.1) following the bioinformatics SOP using the medaka
554 method.

555 **Quality control of assembled genomes**

556 Quast (v5.0.2) was used to compare the assembled genomes to the most closely related
557 publicly available ASFV assembly according to BLAST alignment (MN715134.1)²¹. Samples
558 where both WGS and tiled sequencing were used were compared for overall structure using
559 nucmer (v4.0.0beta2)³⁶.

560 **Phylogeny**

561 The phylogeny analysis was limited to the tiled genomes, as these were the most accurate
562 assemblies, and publicly available genomes. These were aligned using Mafft (v7.467)³⁷ and
563 maximum likelihood trees constructed using iqtree (v2.0.5)³⁸.

564

565 **Acknowledgments**

566 We would like to thank the Bureau of Animal Industry and Milagros Mananggit for providing
567 us access to the valuable ASFV blood samples. We would also like to thank Central Luzon
568 State University and Clarissa Yvonne Domingo and Virginia Venturina and their families for
569 their amazing hospitality during all our visits to the Philippines.

570 We acknowledge financial support from the BBSRC Institute Strategic Programme grant
571 funding to The Roslin Institute (BBS/E/D/20241866, BBS/E/D/20002172, and
572 BBS/E/D/20002174) and BBSRC / Newton Fund Swine and Poultry research initiative grant
573 (BB/R013187/1).

574 **Author Contributions**

575 Outlined the study AW, NC, IV, CYJD, CTB; collected and provided samples RGM, MRM,
576 CYJD; performed experiments AW, NC, CN, IV, RP, LCC, TGB, and CTB; analyzed data
577 AW, NC, SL, and CTB; interpreted data AW, NC, CN, SL, VMV, CYJD and CTB; wrote
578 manuscript, AW and CTB, with contribution of other authors.

579 **Competing Interests Statement**

580 The authors declare no competing interests.

581 References

- 582 1 Blome, S., Franzke, K. & Beer, M. African swine fever – A review of current
583 knowledge. *Virus Research* **287**, 198099, doi:10.1016/j.virusres.2020.198099 (2020).
- 584 2 Sánchez-Vizcaíno, J. M., Mur, L., Gomez-Villamandos, J. C. & Carrasco, L. An
585 Update on the Epidemiology and Pathology of African Swine Fever. *Journal of*
586 *Comparative Pathology* **152**, 9-21, doi:10.1016/j.jcpa.2014.09.003 (2015).
- 587 3 Jori, F. *et al.* Review of the sylvatic cycle of African swine fever in sub-Saharan Africa
588 and the Indian ocean. *Virus Res* **173**, 212-227, doi:10.1016/j.virusres.2012.10.005
589 (2013).
- 590 4 Niederwerder, M. C. *et al.* Infectious Dose of African Swine Fever Virus When
591 Consumed Naturally in Liquid or Feed. *Emerg Infect Dis* **25**, 891-897,
592 doi:10.3201/eid2505.181495 (2019).
- 593 5 Eustace Montgomery, R. On A Form of Swine Fever Occurring in British East Africa
594 (Kenya Colony). *Journal of Comparative Pathology and Therapeutics* **34**, 159-191,
595 doi:[https://doi.org/10.1016/S0368-1742\(21\)80031-4](https://doi.org/10.1016/S0368-1742(21)80031-4) (1921).
- 596 6 Tian, X. & von Cramon-Taubadel, S. Economic consequences of African swine fever.
597 *Nature Food* **1**, 196-197, doi:10.1038/s43016-020-0061-6 (2020).
- 598 7 Penrith, M. L. Current status of African swine fever. *CABI Agriculture and Bioscience*
599 **1**, 11, doi:10.1186/s43170-020-00011-w (2020).
- 600 8 Mighell, E. & Ward, M. P. African Swine Fever spread across Asia, 2018-2019.
601 *Transbound Emerg Dis* **68**, 2722-2732, doi:10.1111/tbed.14039 (2021).
- 602 9 Gaudreault, N. N., Madden, D. W., Wilson, W. C., Trujillo, J. D. & Richt, J. A. African
603 Swine Fever Virus: An Emerging DNA Arbovirus. *Front Vet Sci* **7**, 215,
604 doi:10.3389/fvets.2020.00215 (2020).
- 605 10 Sauter-Louis, C. *et al.* Joining the club: First detection of African swine fever in wild
606 boar in Germany. *Transbound Emerg Dis* **68**, 1744-1752, doi:10.1111/tbed.13890
607 (2021).
- 608 11 Bastos, A. D. *et al.* Genotyping field strains of African swine fever virus by partial p72
609 gene characterisation. *Arch Virol* **148**, 693-706, doi:10.1007/s00705-002-0946-8
610 (2003).
- 611 12 Quembo, C. J., Jori, F., Vosloo, W. & Heath, L. Genetic characterization of African
612 swine fever virus isolates from soft ticks at the wildlife/domestic interface in
613 Mozambique and identification of a novel genotype. *Transbound Emerg Dis* **65**, 420-
614 431, doi:10.1111/tbed.12700 (2018).
- 615 13 Boshoff, C. I., Bastos, A. D., Gerber, L. J. & Vosloo, W. Genetic characterisation of
616 African swine fever viruses from outbreaks in southern Africa (1973-1999). *Vet*
617 *Microbiol* **121**, 45-55, doi:10.1016/j.vetmic.2006.11.007 (2007).
- 618 14 Achenbach, J. E. *et al.* Identification of a New Genotype of African Swine Fever Virus
619 in Domestic Pigs from Ethiopia. *Transbound Emerg Dis* **64**, 1393-1404,
620 doi:10.1111/tbed.12511 (2017).
- 621 15 Malogolovkin, A. & Kolbasov, D. Genetic and antigenic diversity of African swine
622 fever virus. *Virus Res* **271**, 197673, doi:10.1016/j.virusres.2019.197673 (2019).
- 623 16 Netherton, C. L., Connell, S., Benfield, C. T. O. & Dixon, L. K. The Genetics of Life
624 and Death: Virus-Host Interactions Underpinning Resistance to African Swine Fever,
625 a Viral Hemorrhagic Disease. *Front Genet* **10**, 402, doi:10.3389/fgene.2019.00402
626 (2019).
- 627 17 Forth, J. H., Forth, L. F., Blome, S., Höper, D. & Beer, M. African swine fever whole-
628 genome sequencing—Quantity wanted but quality needed. *PLOS Pathogens* **16**,
629 e1008779, doi:10.1371/journal.ppat.1008779 (2020).
- 630 18 Zhu, Z. *et al.* Homologous recombination shapes the genetic diversity of African
631 swine fever viruses. *Veterinary Microbiology* **236**, 108380,
632 doi:<https://doi.org/10.1016/j.vetmic.2019.08.003> (2019).

- 633 19 Jia, L. *et al.* Nanopore sequencing of African swine fever virus. *Sci China Life Sci* **63**,
634 160-164, doi:10.1007/s11427-019-9828-1 (2020).
- 635 20 O'Donnell, V. K. *et al.* Rapid Sequence-Based Characterization of African Swine
636 Fever Virus by Use of the Oxford Nanopore MinION Sequence Sensing Device and a
637 Companion Analysis Software Tool. *J Clin Microbiol* **58**, doi:10.1128/JCM.01104-19
638 (2019).
- 639 21 Olasz, F. *et al.* Short and Long-Read Sequencing Survey of the Dynamic
640 Transcriptomes of African Swine Fever Virus and the Host Cells. *Front Genet* **11**,
641 758, doi:10.3389/fgene.2020.00758 (2020).
- 642 22 Gurevich, A., Saveliev, V., Vyahhi, N. & Tesler, G. QUAST: quality assessment tool
643 for genome assemblies. *Bioinformatics* **29**, 1072-1075,
644 doi:10.1093/bioinformatics/btt086 (2013).
- 645 23 O'Donnell Vivian, K. *et al.* Rapid Sequence-Based Characterization of African Swine
646 Fever Virus by Use of the Oxford Nanopore MinION Sequence Sensing Device and a
647 Companion Analysis Software Tool. *Journal of Clinical Microbiology* **58**, e01104-
648 01119, doi:10.1128/JCM.01104-19 (2021).
- 649 24 Fischer, M., Huhr, J., Blome, S., Conraths, F. J. & Probst, C. Stability of African
650 Swine Fever Virus in Carcasses of Domestic Pigs and Wild Boar Experimentally
651 Infected with the ASFV "Estonia 2014" Isolate. *Viruses* **12**, doi:10.3390/v12101118
652 (2020).
- 653 25 Gallardo, C. *et al.* Attenuated and non-haemadsorbing (non-HAD) genotype II African
654 swine fever virus (ASFV) isolated in Europe, Latvia 2017. *Transbound Emerg Dis* **66**,
655 1399-1404, doi:10.1111/tbed.13132 (2019).
- 656 26 Gallardo, C. *et al.* Genetic variation among African swine fever genotype II viruses,
657 eastern and central Europe. *Emerging infectious diseases* **20**, 1544-1547,
658 doi:10.3201/eid2009.140554 (2014).
- 659 27 Quick, J. *et al.* Multiplex PCR method for MinION and Illumina sequencing of Zika
660 and other virus genomes directly from clinical samples. *Nature Protocols* **12**, 1261-
661 1276, doi:10.1038/nprot.2017.066 (2017).
- 662 28 Sievers, F. *et al.* Fast, scalable generation of high-quality protein multiple sequence
663 alignments using Clustal Omega. *Mol Syst Biol* **7**, 539, doi:10.1038/msb.2011.75
664 (2011).
- 665 29 Ye, J. *et al.* Primer-BLAST: A tool to design target-specific primers for polymerase
666 chain reaction. *BMC Bioinformatics* **13**, 134, doi:10.1186/1471-2105-13-134 (2012).
- 667 30 Kolmogorov, M., Yuan, J., Lin, Y. & Pevzner, P. A. Assembly of long, error-prone
668 reads using repeat graphs. *Nature Biotechnology* **37**, 540-546, doi:10.1038/s41587-
669 019-0072-8 (2019).
- 670 31 De Coster, W., D'Hert, S., Schultz, D. T., Cruts, M. & Van Broeckhoven, C.
671 NanoPack: visualizing and processing long-read sequencing data. *Bioinformatics* **34**,
672 2666-2669, doi:10.1093/bioinformatics/bty149 (2018).
- 673 32 Li, H. Minimap2: pairwise alignment for nucleotide sequences. *Bioinformatics* **34**,
674 3094-3100, doi:10.1093/bioinformatics/bty191 (2018).
- 675 33 Li, H. *et al.* The Sequence Alignment/Map format and SAMtools. *Bioinformatics* **25**,
676 2078-2079, doi:10.1093/bioinformatics/btp352 (2009).
- 677 34 Quinlan, A. R. & Hall, I. M. BEDTools: a flexible suite of utilities for comparing
678 genomic features. *Bioinformatics* **26**, 841-842, doi:10.1093/bioinformatics/btq033
679 (2010).
- 680 35 Silva, G. G. *et al.* Combining de novo and reference-guided assembly with
681 scaffold_builder. *Source Code Biol Med* **8**, 23-23, doi:10.1186/1751-0473-8-23
682 (2013).
- 683 36 Marçais, G. *et al.* MUMmer4: A fast and versatile genome alignment system. *PLOS*
684 *Computational Biology* **14**, e1005944, doi:10.1371/journal.pcbi.1005944 (2018).
- 685 37 Katoh, K., Misawa, K., Kuma, K. i. & Miyata, T. MAFFT: a novel method for rapid
686 multiple sequence alignment based on fast Fourier transform. *Nucleic Acids*
687 *Research* **30**, 3059-3066, doi:10.1093/nar/gkf436 (2002).

688 38 Minh, B. Q. *et al.* IQ-TREE 2: New Models and Efficient Methods for Phylogenetic
689 Inference in the Genomic Era. *Molecular Biology and Evolution* **37**, 1530-1534,
690 doi:10.1093/molbev/msaa015 (2020).
691

692 **Figure Legends**

693 **Figure 1**

694 A) DNA was extracted from blood and sequenced with Nanopore's LSK109 on an m1kb
695 before analysis and assembly using Flye and polishing with medaka. B) Read length
696 histograms for the dataset demonstrating total throughput (blue) and ASFV reads throughput
697 (orange) C) Normalized counts by dataset of reads for total throughput (blue) and ASFV
698 reads throughput (orange). D) Throughput over time for total read count (blue) and ASFV
699 read count (orange).

700 **Figure 2**

701 A) Design of the tiled primer scheme for ASFV with ~7kb amplicons and ~1kb overlaps. B)
702 Predicted primer binding in correct region for representative ASFV genotypes. C) Workflow
703 with extraction from blood, PCR amplification of primer pools, pooling, sequencing and
704 bioinformatic analysis D) Coverage of one sample (PHL-3142) amplified with either evenly
705 represented primer pairs (purple) or optimized proportions of primer pairs (green). E)
706 Tapestation capillary electrophoresis of amplified pools of two different samples, the low
707 quality PHL-126 and the high quality PHL-261, and statistics of the resulting assemblies of
708 each of these. F) Coverage of amplicons using optimized primer concentrations for the two
709 samples from figure 1E. G) Impact of post-amplification DIN on proportion of reads <3kb in
710 length, essentially wasted sequencing capacity, using R9.4 flow cells and LSK-109
711 (magenta) or R10.4 and LSK-110 (blue). Semilog fit analysis shows an R squared
712 correlation of 0.6420 or 0.7244, for R9.4_109 and R10.4_110, respectively. H) Association
713 between overall throughput >3kb and number of gaps in final assembly using HAC
714 (black/bold) and SAC (grey/faint). A log-log analysis shows an R squared correlation of
715 0.9680 and 0.9358 for HAC and SAC, respectively. PHL-126 is highlighted in orange and
716 PHL-261 in blue. I) Assembly accuracy based on proportion of mismatches against
717 reference (MN715134.1), with lines showing Q40 and Q50 PHRED scores. J) Assembly

718 accuracy based on proportion of indels against reference (MN715134.1), with lines showing
719 Q30 and Q40 PHRED scores. A&C Created with BioRender.com

720 **Figure 3**

721 A) Directed acyclic graph showing the steps the Lilo pipeline takes during assembly. The
722 graph has been simplified to show assembly of a genome containing 2 amplicons
723 (amplicon_01 and amplicon_n) for a single sample. B) Quast results for genomes
724 sequenced with tiled amplicons or from shotgun sequencing on R9.4 flow cells using SQK-
725 LSK109. Note PHL-10 and PHL-30 were sequenced with an earlier version of the primer
726 scheme with one primer different and are expected to have a 25bp gap C) Nucmer
727 alignment of PHL-261 genomes assembled from WGS or Lilo tiled assembly. D) Nucmer
728 alignment of PHL-237 genomes assembled from WGS or Lilo tiled assembly. Figure 4

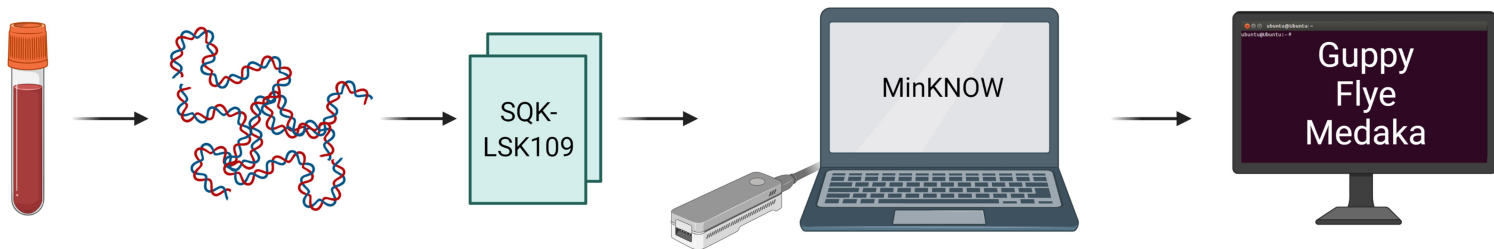
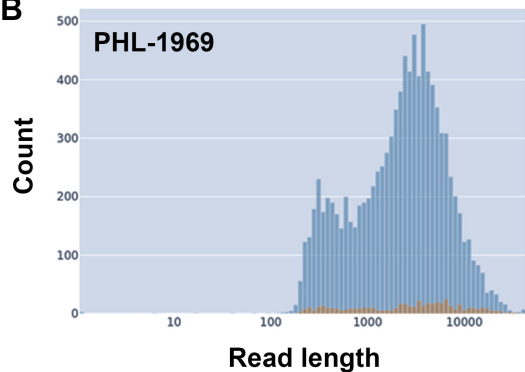
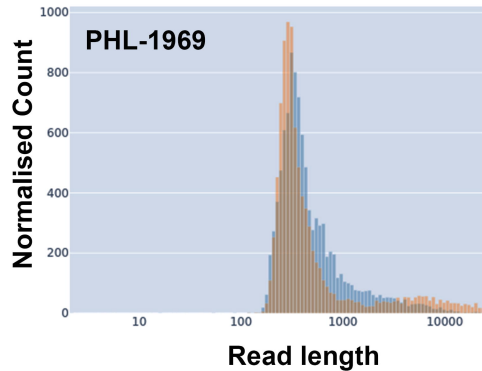
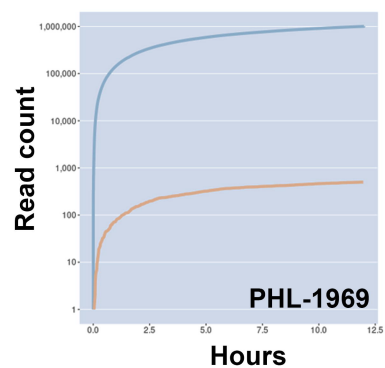
729 B) IGV image showing alignment of genomes assembled with Lilo or Artic (top) and
730 assemblies and reads for a single sample (PHL-10) aligned to a reference (MN715134.1).
731 This image shows a likely real indel present in all assemblies and supported by the reads. C)
732 as in B, but showing an indel common in Lilo assemblies and missing in Artic assemblies
733 and the reference. D) as in B, but showing a long homopolymer with poor consensus from
734 the reads and inconsistent results in assemblies. E, F & G) Examples of indels specific to the
735 Artic pipeline assemblies which do not agree with the reference.

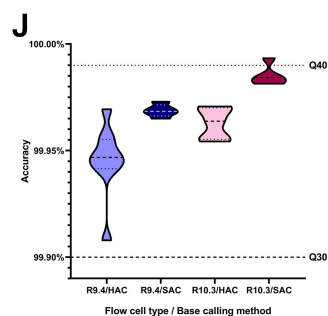
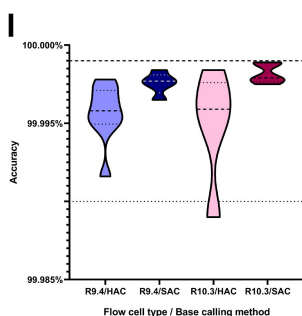
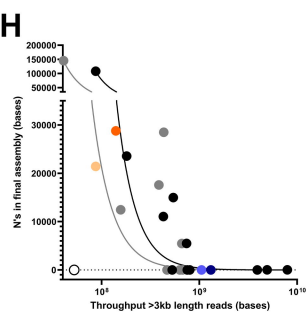
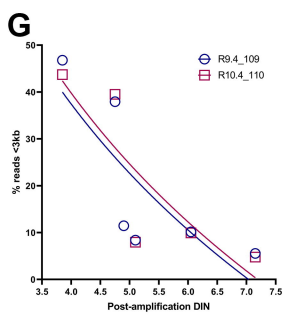
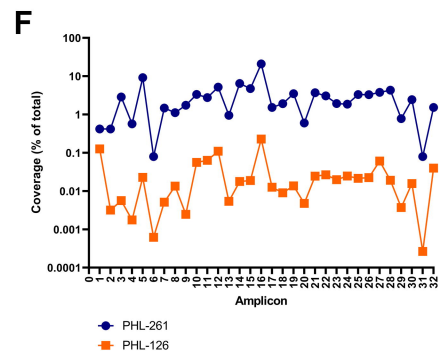
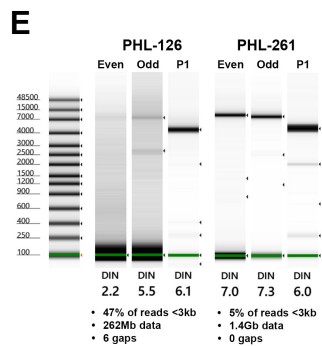
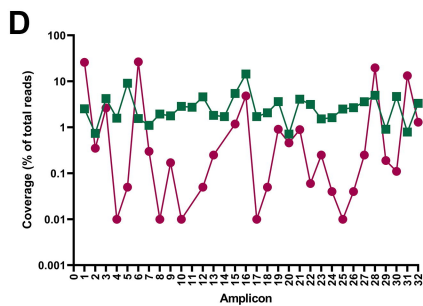
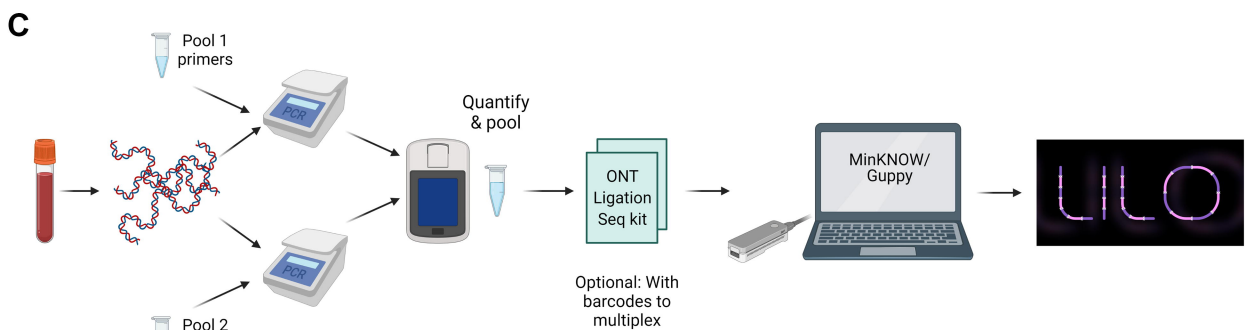
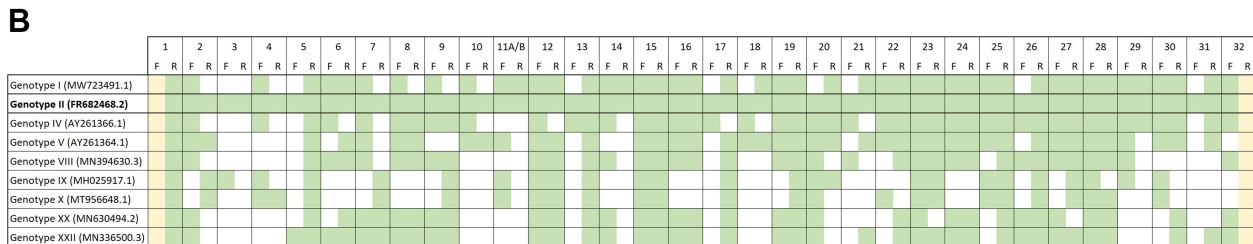
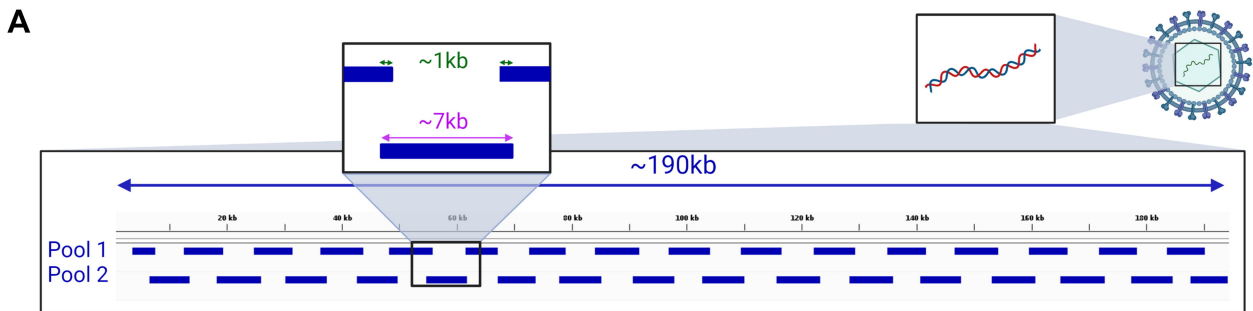
736 **Figure 5**

737 Maximum likelihood trees for our R9.4/SQK-LSK109 genomes and A) all available ASFV
738 genomes downloaded from NCBI (09/11/2021) or B) those specifically clustering with
739 genotype II.

740

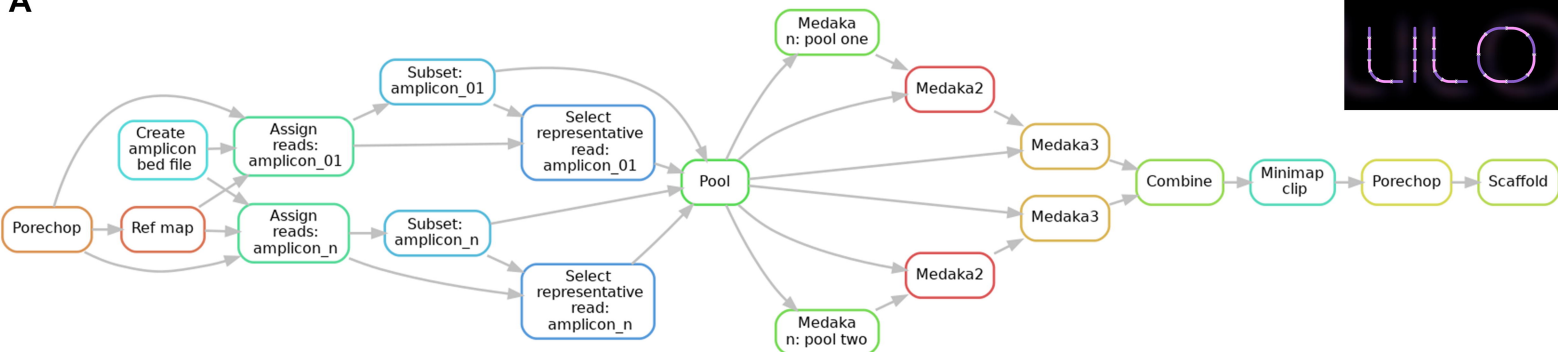
741

A**B****C****D**





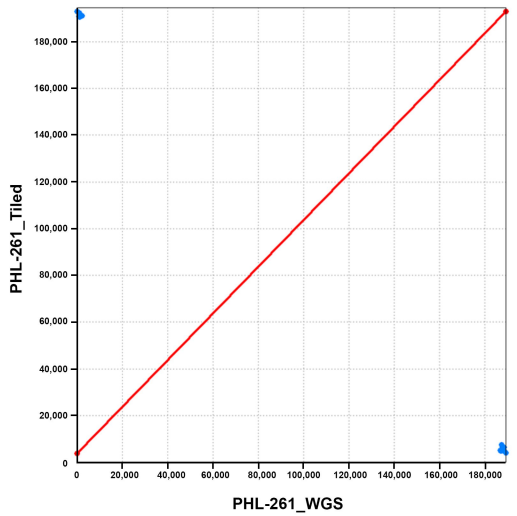
A



B

					Mismatches/ 100kb	Indels/ 100kb	% of genome N's	Post-amp DIN	% reads <3kb	Total Mismatches	Total Indels	Assembled Genome Length
Whole genome sequences												
PHL-100	109	R9.4	HAC	LILO	63.54	578.23	0			120	1,092	191,202
PHL-237	109	R9.4	HAC	LILO	17.90	102.12	0			34	194	201,056
PHL-261	109	R9.4	HAC	LILO	10.04	199.26	0			19	377	189,291
PHL-2842	109	R9.4	HAC	LILO	9.44	153.74	0			18	293	192,401
PHL-1969	109	R9.4	HAC	LILO	18.89	81.33	0			36	155	194,709
Tiled - ARTIC versus LILO												
PHL-10	109	R9.4	HAC	LILO	4.20	24.30	0.01		14.65	8	46	189,551
PHL-10	109	R9.4	HAC	ARTIC	1.60	38.40	2.49		14.65	3	73	194,629
PHL-30	109	R9.4	HAC	LILO	2.60	31.70	0.01		25.08	5	60	189,557
PHL-30	109	R9.4	HAC	ARTIC	1.60	38.40	2.49		25.08	3	73	194,635
PHL-3142	109	R9.4	HAC	LILO	5.30	37.40	0	6.70	16.71	10	71	189,861
PHL-3142	110	R9.4	HAC	LILO	3.20	71.10	0	4.90	11.46	6	135	190,114
PHL-3142	110	R9.4	HAC	ARTIC	1.10	38.40	2.40	6.70	16.71	2	73	194,631
Tiled - 109 / R9.4 vs 110 / R10.3												
PHL-126	109	R9.4	HAC	LILO	3.70	42.60	0	2.40	24.37	7	81	189,902
PHL-126	109	R9.4	SAC	LILO	2.60	25.20	0	2.40	23.86	5	48	189,909
PHL-126	110	R10.3	HAC	LILO	4.30	24.20	17.84	3.85	46.80	7	39	161,294
PHL-126	110	R10.3	SAC	LILO	1.30	9.40	11.28	3.85	43.72	2	14	190,035
PHL-233	109	R9.4	HAC	LILO	4.80	49.90	12.42	1.80	39.71	8	83	189,872
PHL-233	109	R9.4	SAC	LILO	2.40	31.90	6.57	1.80	39.50	4	53	189,520
PHL-233	110	R10.3	HAC	LILO	11.00	25.70	56.96	4.75	37.94	9	21	190,074
PHL-233	110	R10.3	SAC	LILO	2.20	6.70	76.42	4.75	39.52	1	3	190,087
PHL-237	109	R9.4	HAC	LILO	8.10	47.20	2.98	5.15	18.92	15	87	184,406
PHL-237	109	R9.4	SAC	LILO	2.20	22.80	2.88	5.15	18.62	4	42	189,818
PHL-237	110	R10.3	HAC	LILO	1.60	28.40	0	6.05	10.16	3	54	190,090
PHL-237	110	R10.3	SAC	LILO	1.00	10.50	0	6.05	9.94	2	20	189,962
PHL-2607	109	R9.4	HAC	LILO	2.20	40.90	5.84	1.35	41.08	4	73	189,585
PHL-2607	109	R9.4	SAC	LILO	3.50	23.80	9.28	1.35	40.69	6	41	189,503
PHL-2607	110	R10.3	HAC	LILO	3.70	23.50	9.28	5.10	8.40	6	38	161,518
PHL-2607	110	R10.3	SAC	LILO	2.50	12.40	15.00	5.10	7.95	4	20	189,995
PHL-261	109	R9.4	HAC	LILO	4.70	43.70	0	6.15	11.37	9	83	189,878
PHL-261	109	R9.4	SAC	LILO	1.60	22.60	0	6.15	10.95	3	43	189,881
PHL-261	110	R10.3	HAC	LILO	3.20	21.10	0	7.15	5.55	6	40	189,886
PHL-261	110	R10.3	SAC	LILO	2.10	8.40	0	7.15	4.78	4	16	189,933

C



D

